ELSEVIER

Journal of Nuclear Materials 258–263 (1998) 1033–1039

journal of nuclear materials

Deformation and fracture of Cu alloy–stainless steel layered structures under dynamic loading

J.H. McCoy [a,*], A.S. Kumar [a], J.F. Stubbins [b]

[a] *Department of Nuclear Engineering, University of Missouri at Rolla, Rolla, MO 65401, USA*
[b] *Department of Nuclear Engineering, University of Illinois at Urbana-Champaign, Urbana, IL 61801, USA*

Abstract

Fracture resistance of the current ITER first wall configuration, a copper alloy–stainless steel layered structure, is a major design issue. The question of dynamic crack propagation into and through the first wall structure is examined using dynamic finite element modeling (FEM). Several layered configurations that incorporate both strain and frictional energy dissipation during the fracture process are considered. With fixed overall specimen geometry, the energy required to extend a precrack is examined as a function of material properties, and the layer structure. It is found that the crack extension energies vary dramatically with the fracture strain of materials, and to a much lesser extent with the number of layers. In addition, it is found that crack propagation through the lower ductility copper alloy layer may be deflected at the stainless steel–copper interface and not result in total fracture of the structure. Although the total energy required is affected only to a small degree by the interface properties, the time to extend the precrack is strongly affected. By making proper selections of the interface and the layered material, crack propagation rates and the possibility of full fracture can be substantially reduced.

1. Introduction

Layered composite structures have been selected for a variety of plasma facing and primary wall applications in ITER and other fusion devices. These structures will be used for components, including the primary wall, the limiters, and the divertor, that will experience severe service conditions. For ITER, these structures are slated to employ IG 316LN stainless steel as a structural material. One of three possible copper alloys, CuA125, CuNiBe or CuCrZr, is to be bonded to the steel for efficient heat removal of the high thermal fluxes emanating from the plasma. One of several possible plasma facing materials will be laminated on top of the copper alloy. Current possible plasma facing materials are Be, W or carbon–carbon composites. The methods for bonding the layers in these structures, and their performance under a variety of mechanical and thermal loading conditions has been the topic of several recent and ongoing studies by the ITER partners [1–5].

The fabrication process must ensure an adequate bond, preserve the bulk material properties of the components of the composite, and be viable for large (1 m × 1 m) complex structures. Hot isostatic pressing (HIP) has been selected to accomplish this bonding. Temperature, pressure and duration of this process is still under investigation, but reasonable bonds between copper alloys and 316L stainless steel can be produced for the following HIP conditions: $T = 920$–$980°C$, $P = 102$ MPa, and $t = 2$ h. The precipitation strengthened copper alloys (CuNiBe and CuCrZr) require an additional heat treatment to develop a proper precipitate structure, usually an additional heat treatment for 3–5 h at 380–500°C, depending on the alloy and the desired size and distribution of the precipitates.

While there have been substantial efforts to investigate these structures for mechanical properties, primarily to establish the strength and integrity of the bond, little attention has been paid to dynamic fracture issues with such structures. Dynamic loading is often used as a

* Corresponding author. Address: 111, Rolla, MO 65401 USA. Tel.: +1-573 341 6551; fax: +1-573 341 6309; e-mail: jhmccoy@umr.edu.

0022-3115/98/$19.00
PII: S0022-3115(98)00277-3

method of assessing lower bound fracture resistance since dynamic fracture usually tends to result in less energy absorption than standard fracture toughness tests performed at more moderate strain rates. In fact, there has been very little consideration of dynamic fracture of laminate structures other than some early considerations regarding potential strengthening and fracture resistance effects [6]. The current work examines the dynamic loading effects in Glidcop and stainless steel layered structures.

2. Modeling and computational approach

All modeling was performed using a dynamic explicit-integration finite element code, ABAQUS Explicit, from Hibbit, Karlsson and Sorensen Corporation [7]. Some portions of the input files were generated using IDEAS-SDRC Version VI [8]. ABAQUS Explicit uses a dynamic analysis procedure that implements an explicit-integration rule with the use of diagonal mass matrices [7]. The code integrates through time using many small, stable time increments. The time increment scheme in ABAQUS is fully automatic and requires no user intervention. The use of small increments (dictated by a stability limit) is advantageous in that it allows the solution to proceed without iterations and without requiring tangent stiffness matrices. It also simplifies the treatment of contact.

The stable time increment decreases exponentially with decreasing element size. Therefore, the total CPU time usually increases exponentially with the refinement of the mesh and linearly with the number of elements in the model. The explicit procedure is ideally suited for analyzing high speed dynamic events like those found in impact testing.

ABAQUS Explicit contains an elastic-plastic material model that allows crack extension to be modeled by deleting elements from the mesh. ABAQUS treats crack extension by calculating an element-averaged strain and then deleting elements in the mesh when any element reaches an input defined plastic fracture strain (ε_f^{pl}). In order for this deletion of elements to produce stable results, the stress state of the damaged element must be reduced to zero by the time of fracture. ABAQUS accomplishes this by applying a damage level parameter to the material prior to fracture. This damage parameter is used to degrade the stress state as well as the elastic moduli. The damage value of any element is zero until the strain in the element exceeds a user-defined offset fracture strain (ε_0^{pl}). The damage (D) in an element can range from zero (no damage) to one (failed) and is calculated from the equivalent plastic strain as follows:

$$D = \frac{\left(\varepsilon^{pl} - \varepsilon_0^{pl}\right)}{\left(\varepsilon_f^{pl} - \varepsilon_0^{pl}\right)}.$$

When the damage reaches a value of one, the element is deleted from the mesh and a crack is formed or extended.

All of the dynamic modeling of fracture in this paper is focused on drop tower impact tests. In these tests, a specimen containing a precrack in the bottom layer is impacted from the top by a striker. A user-defined FORTRAN subroutine has been written to model the dynamic crack propagation. This subroutine is called by ABAQUS instead of the ABAQUS material fracture model and uses the same mechanism for modeling crack initiation and propagation as the ABAQUS model with the exception of when the damage (D) is incremented. A hydrostatic stress, averaged over the three principal stresses in the element, is used to determine if an element is under tensile or compressive loading. If the hydrostatic stress is positive, D is allowed to increase in that time increment. Otherwise, no further damage can result.

The finite element model used is of a two-dimensional specimen (1 cm × 5.4 cm). The model contained a sharp precrack to a depth of 0.25 cm (one-quarter of the specimens overall thickness) at the mid-length. The precrack provides a direct indication of energies to propagate the crack without the influence from crack initiation. In order to determine the relative fracture resistance of multilayered structures, the amount of energy required to extend the precrack by 0.025 cm (the smallest mesh size) is compared for all cases investigated.

The specimens comprised of two to five layers such that the bottom half of the specimen (with the precrack) was a single material (either Glidcop or stainless steel) and the top half was either a single layer, divided into two or four layers of the other material (either stainless steel or Cu alloy). Two types of interfaces were assumed: Either the layers were ''tied'' together, or they interacted via frictional forces. In the former case, no direct energy was dissipated due to adhesion between the layers, while in the latter case, substantial energy could be dissipated in the form of frictional sliding.

The materials properties for these studies were taken from those used successfully in finite element modeling (FEM) of Glidcop to stainless steel laminate mechanical properties test programs [4]. The values are shown in Table 1.

Table 1
Material properties used to model Glidcop and stainless steel

Material	Yield stress (MPa)	Young's modulus (GPa)	Hardening modulus (GPa)	Poisson's ratio
Glidcop	410	130	11.0	0.343
Stainless steel	207	200	8.0	0.285

3. Results and discussion

The results and discussion of the findings are detailed in two separate areas: Deformation and fracture energy, and crack propagation.

3.1. Deformation and fracture energy

The total energy in deformation and fracture is the sum of two predominant components, the strain energy and the friction energy. It is important to note that the values of the strain energies and the frictional energies are of similar order, both play significant roles in the total energy absorption behavior, except when the coefficient of friction is set to zero, making the frictional energy term disappear.

Figs. 1–3 show the total energy absorbed during extension of a precrack by 0.025 cm in four different structures. Each structure is represented by a two letter code described below and in Table 2. The letters S and D stand for low (0.02) and high (0.50) fracture strain stainless steels, while B and M stand for low (0.02) and higher (0.08) fracture strain Glidcop alloys. Table 2 also shows the offset fracture strains ($\varepsilon_0^{\mathrm{pl}}$) of each material used in the modeling. The first letter represents the top layer(s) while the second letter represents the bottom layer which is 0.5 cm thick and is precracked to a depth of 0.25 cm. The length of the layers is 5.4 cm and the total thickness including top and bottom layers is 1 cm. All of the computations are performed for plane strain conditions. The layered structure is impacted from the top by a striker of mass 10 kg with a kinetic energy of 500 J.

The layered structures SB and DB shown on the left side in Fig. 1 absorb approximately the same amounts of energy (0.7 J) when the top and bottom layers (each 0.5 cm wide) are tied together. The same conclusion can be drawn when the top is divided equally into four layers (5 layers including the 0.5 cm thick bottom layer). Each of the four layers is 0.125 cm thick and slides on the adjoining layers with a coefficient of friction (μ) equal to unity. The total energy absorbed for both SB and DB increases from 0.7 J for the tied structures to approximately 1.7 J for the layered structure, with most of the increase coming from frictional energy losses between the layers. It is therefore concluded that even a substantial increase in the fracture strain of the top layer(s) from 0.02 to 0.50 has little effect on the total energy absorbed for crack extension in the bottom layer. In addition, the layered structures appear to inhibit crack extension by absorbing a large fraction of the energy in frictional losses.

Similar conclusions can be drawn from the fracture of two other layered structures SM and DM shown on the right side of Fig. 1. Compared to the layered structures SB and DB, the material of the bottom layer in SM and DM has a higher fracture strain of 0.08. In the case of tied structures (2 layers), the total absorbed energy for both structures increases to approximately 4.3 J from 0.7 J for the structures SB and DB. Again, the fracture strain (or ductility) of the top layer has little influence on the absorbed energy, and therefore, it is concluded that most of the energy is absorbed near the crack tip in the bottom layer. A higher fracture strain of the bottom precracked layer requires a higher absorbed energy for crack extension.

A comparison of the sliding layered structures of SM and DM in Fig. 1 confirms the conclusions drawn for the tied structures. With five layered structures (four top layers of equal width, 0.0125 cm, and one bottom layer of 0.5 cm width) the total energies absorbed are approximately 4 and 5 J for SM and DM, respectively. Although the top layer(s) in these two cases have substantially different fracture strains (0.02 and 0.50), the total energy absorbed differs only by 25%.

Fig. 2 shows the total energy divided into strain energy and frictional energy in a set of DM layered structures. The tied (rigidly bonded) two layer structure

Table 2
Fracture strains used in ABAQUS model

Material (letter code)	Offset fracture strain ($\varepsilon_0^{\mathrm{pl}}$)	Fracture strain ($\varepsilon_f^{\mathrm{pl}}$)
B (Glidcop)	0.015	0.020
S (stainless steel)	0.015	0.020
M (Glidcop)	0.075	0.080
D (stainless steel)	0.400	0.500

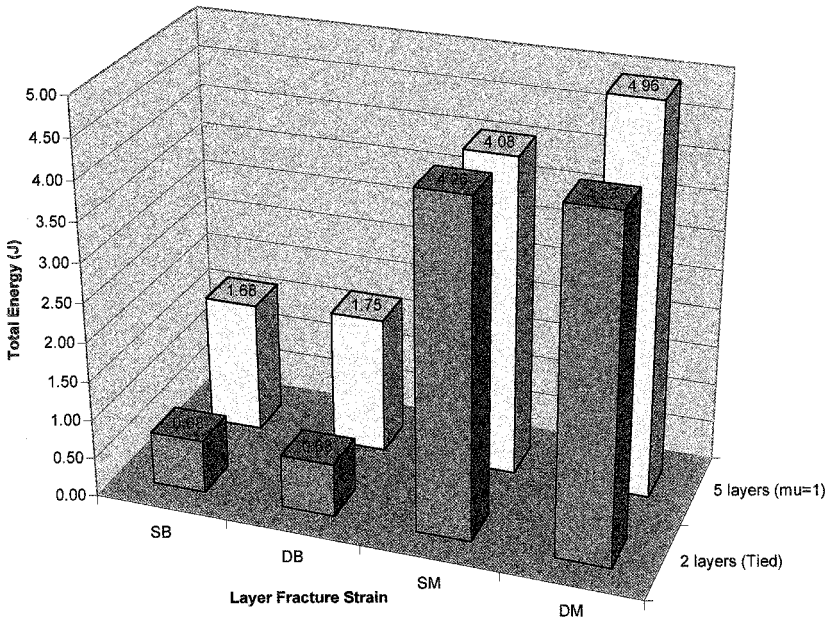

Fig. 1. Total energy dissipated in a layered structure to extend a precrack 0.025 cm deep in the Glidcop layer below the above stainless steel layer(s).

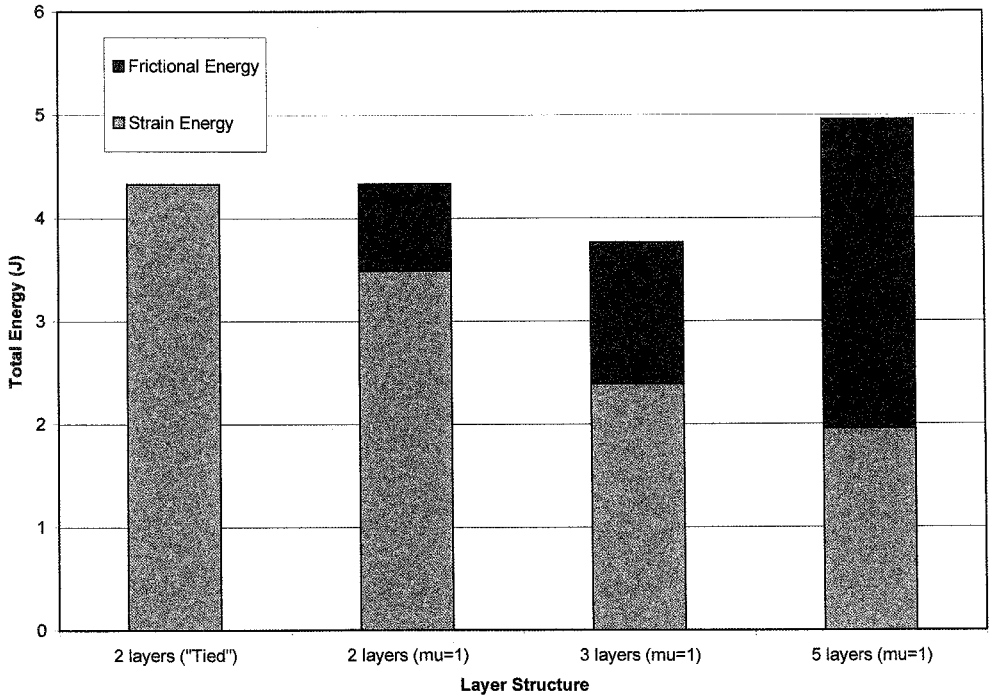

Fig. 2. Total energy (in component form) dissipated in a layered structure to extend a precrack 0.025 cm deep in the Glidcop layer below the above stainless steel layer(s).

had a strain energy of approximately 4.3 J. The layered structures with friction at the interface had a strain energies of 3.5, 2.4 and 2.0 J for the two, three and five layer structures, respectively. Simulations show that the strain energy decreases monotonically with an increase in the number of layers. The layered structures with friction at the interface also dissipate energy in frictional losses. The frictional energies of those structures were 0.9, 1.4 and 3.0 J for the two, three and five layer structures, respectively. The frictional energy exhibits an opposite behavior such that an increase in the number of layers results in an increase in the frictional energy.

The decrease in strain energy is due to the thinner layers approaching a state of plane stress with reduced constraints. These thinner layers do not transfer the load to adjoining layers in comparison to the thicker layers, resulting in a lessening of the strain energy. The increase in frictional energy with the number of layers is due to an increase in the area of frictional surfaces.

3.2. Crack propagation

As shown in Fig. 3, multilayer structures bonded with friction do have an important role in the time necessary to extend a precrack. Compared to the tied case, the frictional multilayer structures cause a significant increase in the time to extend the precrack. Delay in the time for crack extension under dynamic loading has the following implication. Longer the delay, the more deformation is spread in the structure. Larger deflections, rather than faster crack propagation, occur in layered structures due to the larger deformation in the thinner top layers (which carry a significant amount of the load). This creates a reduced state of stress at the crack tip in the bottom layer.

Fig. 4 provides a graphic representation of the crack propagation in the tied model. When the bond at the interface is strong, the relative ductility and mechanical properties of the materials determine the path of crack propagation. A weaker material in the bottom layer will result in the crack advancing to the interface, then turning parallel to the interface and running along it. In contrast, it has been shown that if the materials are of equal strength, then the crack usually propagates through the interface and into the top layer.

4. Conclusions

From the results of a systematic study of the influence of the number of layers and interlayer frictional losses in Glidcop to 316L stainless steel layered structures, the following conclusions can be drawn.

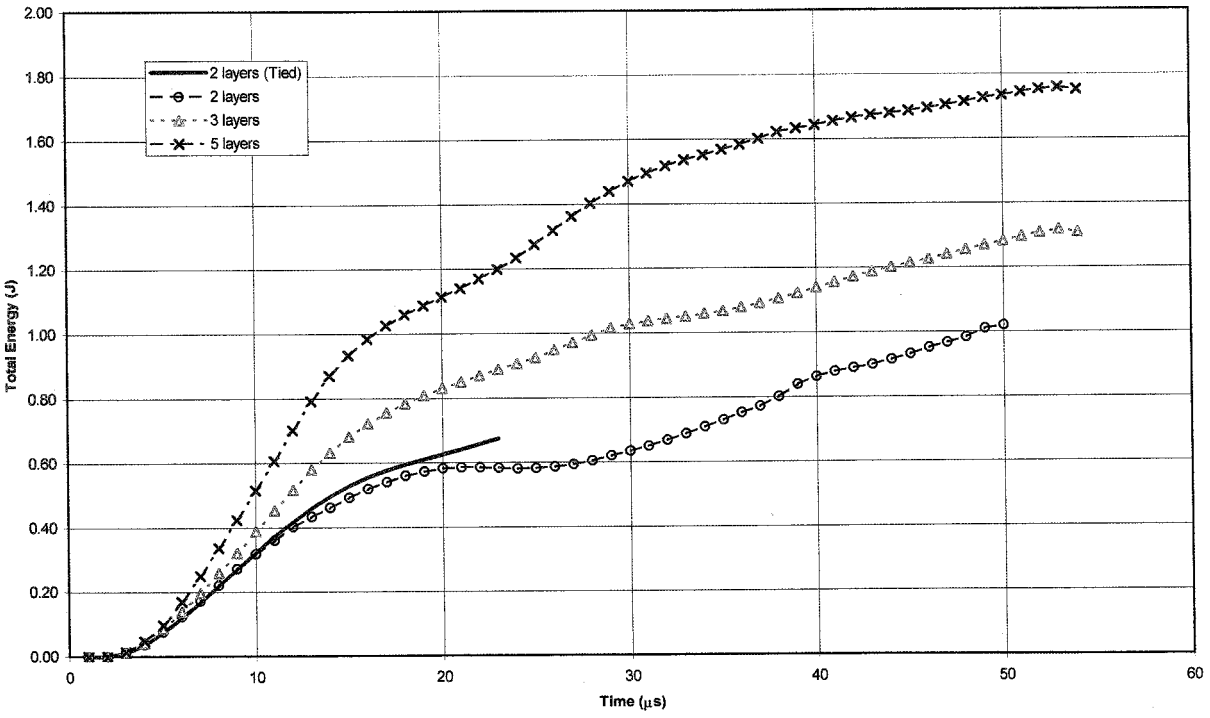

Fig. 3. Total energy dissipated in layered structure to extend precrack 0.025 cm deep in the Glidcop layer below the above stainless steel layer(s). Time required to extend the precrack is substantially increased by multilayer structures.

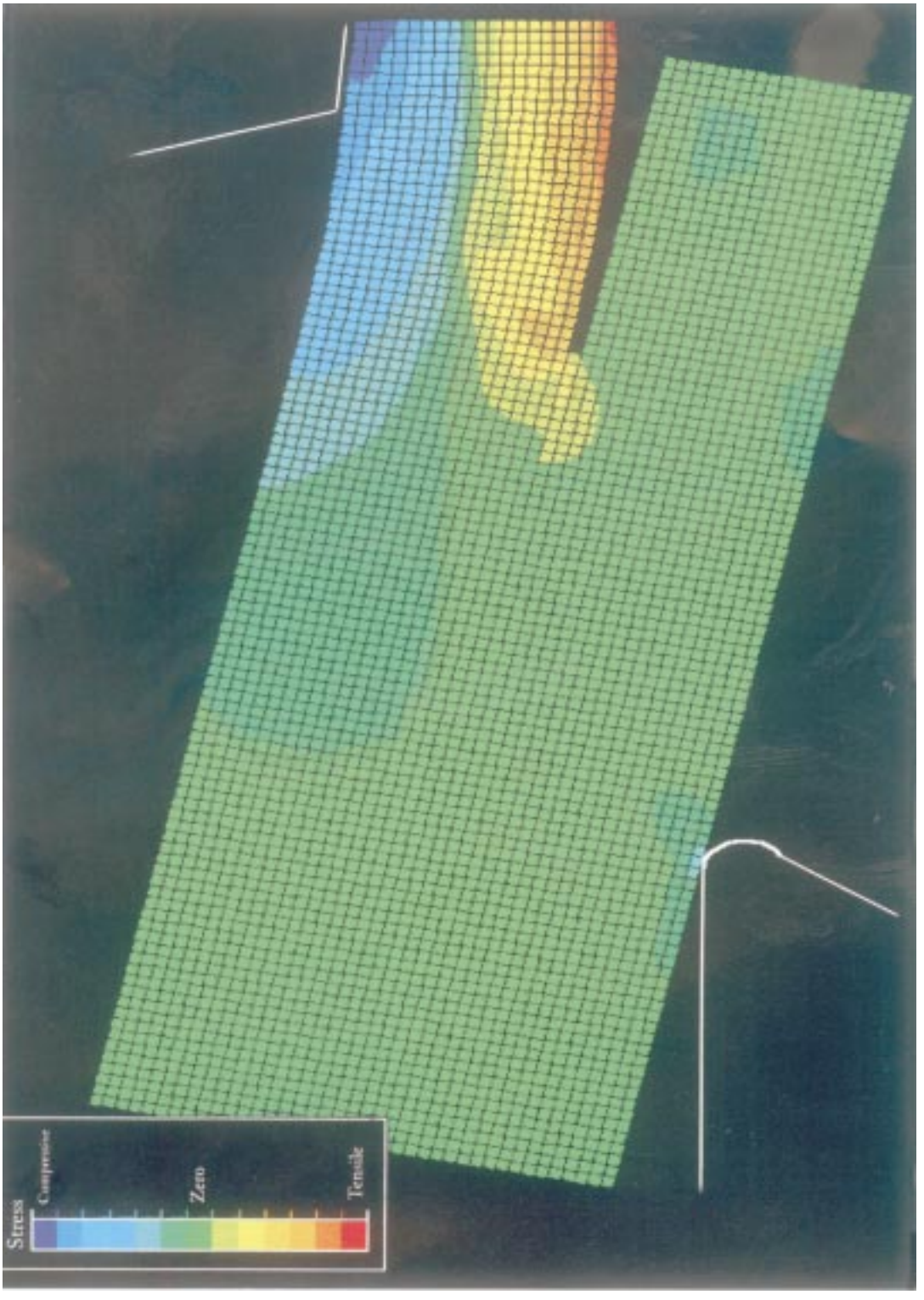

Fig. 4. Graphic representation of crack propagation in the tied model.

1. The total energy dissipated in extending a precrack is controlled by the properties of the material at the crack tip. Of those properties, dynamic fracture strain influences the energy dissipated the most. The fracture strain of the layer(s) other than the precracked layer has a weak influence on the energy dissipation.

2. Layered structures do not increase the total energy dissipated in crack extension significantly. However, they do increase the time required to extend the precrack substantially.

3. The relative material properties of the layers determine the path of crack propagation. If the precracked layer has a sufficiently low fracture strain in comparison with the fracture strain of the top layer, the crack propagates to the interface, turns and runs along the interface. In the reverse situation, however, the precrack in the high fracture strain material propagates across the interface into the low fracture strain material.

Acknowledgements

This was supported, in part, by the US Department of Education under the Graduate Assistantship in Areas of National Needs (GAANN) fellowship program.

References

[1] G. Le Marois, Ch. Dellis, J.M. Gentzbittelm, F. Moret, J. Nucl. Mater. 233–237 (1996) 927–932.
[2] S. Sato, T. Kuroda, T. Kurasawa, K. Furuya, I. Togami, H. Takatsu, J. Nucl. Mater. 233–237 (1996) 940–944.
[3] J.F. Stubbins, et al., Cu-alloys to SS joining techniques assessment, development and recommendation, joint mechanical testing, fracture mechanics and cyclic fatigue tests of Cu/SS and Cu/Be welds, Final Report of US ITER Task T8 (CY1995), ITER Report No. ITER/US/95/IV-BL-20, December 1995.
[4] J.F. Stubbins et al., Cu/SS joining techniques; Development and testing, Final Report of US ITER Task T212 (CY 1996), ITER Report No. ITER/US/97/IV-BL-1, February 1997.
[5] J.F. Stubbins, P. Kurath, D. Drockelman, G.D. Morgan, J. McAfee, G. Li, B.G. Thomas, in: Proceedings of the 16th Symposium on Fusion Engineering, 1996, pp. 174–177.
[6] R.W. Hertzberg, Deformation and Fracture Mechanics of Engineering Materials, Wiley, New York, 1976, pp. 327–335.
[7] Hibbit, Karlsson and Sorenson, Inc., ABAQUS Explicit Users Manual Version 5.5, HKS, 1996.
[8] M.H. Lawry, I-DEAS Master Series Student Guide, Structural Research Dynamics Corporation, 1993.